



An impedance matrix constrained-based method for harmonic emission level estimation

Xian Zheng | Xianyong Xiao | Yang Wang

College of Electrical Engineering, Sichuan University, Chengdu, China

Correspondence

Xian Zheng, Wangjiang Campus, Sichuan University, No.24 South Section 1, Yihuan Road, Chengdu 610065, China.
Email: scuzxx@163.com

Funding information

National Science Foundation of China, Grant/Award Number: #51807126; State Grid Corporation of China Research Program, Grant/Award Number: SGZJDK00DWJS1900033; China Scholarship Council

Summary

The harmonic impedances are important for both utility companies and their customers. The data have many uses, such as estimating harmonic emission levels, designing filters. Complex independent component analysis is a well-accepted method for harmonic impedance estimation. However, a lack of data points for each calculation leads to wrong results. To increase the feasibility of this method, we proposed a constrained complex independent component analysis-based method by adding the essential feature of the harmonic impedance matrix. Thus, the recovered source signals, which are highly consistent with the original source signals can be found when the data quantity for each calculation is little. The method has been verified using simulation studies and extensive field data. The results show that the proposed method can serve as a useful tool to support the harmonic impedance calculation task of utility companies and their customers.

KEY WORDS

constrained complex independent analysis, emission level, harmonic analysis, harmonic impedance, impedance matrix constraint, wind farm

1 | INTRODUCTION

With the innovation of power electronic technology, power electronic converters are widely used in many industrial fields, such as the grid-connected system of renewable energy,¹ HVDC,² and electrical traction railway systems.³ Harmonic pollution is inevitably brought into the power grid, which threatens the security and stability of the power system, increases the energy loss, leads to line overheating, and results in harmonic resonance.⁴ Limiting harmonic emissions from these harmonic pollution sources has become a common industry practice.⁵ To better suppress the harmonic, it is critical to assess the harmonic emission levels for these harmonic sources at the point of common coupling.

After many years' research efforts, two broad approaches to estimating the harmonic equivalent circuit impedance have been proposed. The first approach is an intrusive method,^{6–10} which switches on/off a piece of downstream equipment such as shunt capacitors and lines. The resulting network voltage and current responses are used for impedance estimation. Although it can obtain a reliable result, the disturbance may have a large impact on the networks so the supply side may not permit such operation.^{11,12} The second approach is a non-intrusive method, which can avoid the

List of symbols and abbreviations: PCC, the point of common coupling; ComplexICA, complex independent component analysis; \dot{U}_{pcc} , harmonic voltage at point of common coupling; \dot{I}_{pcc} , harmonic current at point of common coupling; \dot{I}_{u} , harmonic source of utility side; \dot{I}_{c} , harmonic source of customer side; Z_{u} , harmonic impedance of utility side; Z_{u} , harmonic impedance of customer side.

above problem using the natural load variations for harmonic impedance estimation. Therefore, it raises many concerns in the field of harmonic emission level assessment.

Typical non-intrusive methods include fluctuation method,^{13,14} linear regression method,¹⁵⁻¹⁷ random vectors covariance method,¹² Cauchy mixed model-based method,¹⁸ and independent component analysis (ICA) method.¹⁹⁻²³ The fluctuation method and linear regression method are poor in terms of resisting the variation of background harmonic inherently, which usually requires background harmonic source keep constant, and the customer side harmonic source is the dominant harmonic source at PCC. The method based on covariance characteristics of random vectors, which measures the utility harmonic impedance based on the utility harmonic source and the harmonic current at PCC are weakly correlated or independent, it can suppress the influence of background harmonic to some degree. However, it leads to incorrect results when the harmonic impedances of both sides are approximately equal. The Cauchy mixed model-based method¹⁸ overcomes the above problems to some extends. However, the accuracy of this method is based on the statistical characteristics fitting of the measured data. Besides, it can only be used to calculate utility side harmonic impedance, which does not apply to the case that the harmonic impedances of both sides are nearly equal.

Harmonic load fluctuation is composed of fast-varying components and slow-varying components, and the fast-varying components are independent.¹⁹ Therefore, the independent component analysis methods are proposed²⁰⁻²³ based on this principle. These methods are free from the assumption that the customer side harmonic impedance is much large than that of the utility side, which can estimate the harmonic impedance accurately when the background harmonic fluctuates acutely. Nevertheless, the reliability of the ComplexICA mainly depends on the amount of data for each calculation; lack of data may result in the wrongly capturing of the data's statistical characteristics and may lead to local convergence or divergence. Extending the sample time to obtain more recorded data can ensure accuracy. However, the longer the sample time, the bigger the possibility of the harmonic impedance change during the measured period, which results in new errors consequently.

The presented paper studies the influence of the harmonic impedance amplitude ratio between utility and customer side on the harmonic emission level assessment firstly. Then, the drawbacks of the ComplexICA are analyzed, and an impedance matrix constrained-based method is proposed to solve these problems. To limit the optimization direction of ComplexICA and improve the separated performance with little data for each calculation, the inherent properties of the impedance matrix are adopted as prior information of the separated matrix for the constrained complex independent component analysis algorithm. As a result, the recovered signals, which are highly consistent with the original source signals, can be found. Finally, the harmonic impedances of both sides are calculated using the separated matrix. The proposed method is tested using case studies and field data, and its performance has been found acceptable for industry applications.

2 | BASICAL KNOWLEDGEMENT

2.1 | Problem description

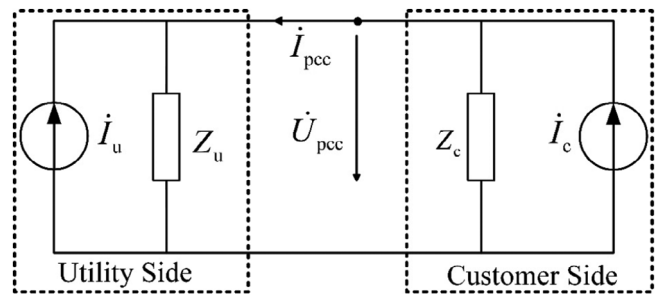
A customer facility consists of both linear and nonlinear loads. At a specific harmonic frequency, the linear part of the customer is equivalent to harmonic impedance, and the nonlinear parts are approximated to a harmonic current source. Thus, a customer facility can be modeled as the Norton equivalent circuit. Meanwhile, the utility side usually contains utility equipment and other customer loads connected to the system, and some of these customers may contain harmonic sources. Hence, the utility side can be also represented by the Norton equivalent circuit. The existing works for harmonic emission level estimation are based on the equivalent circuit shown in Figure 1, where the subscript “h” is omitted for simplification.

According to superposition theory, we have:

$$\begin{cases} \dot{U}_{\text{pcc}} = \frac{Z_c Z_u}{Z_c + Z_u} (\dot{I}_u + \dot{I}_c) \\ \dot{I}_{\text{pcc}} = \frac{Z_c}{Z_c + Z_u} \dot{I}_c - \frac{Z_u}{Z_c + Z_u} \dot{I}_u \end{cases}, \quad (1)$$

where \dot{U}_{pcc} and \dot{I}_{pcc} represent the harmonic voltages and harmonic currents measured at PCC separately. \dot{I}_u and \dot{I}_c represent the equivalent harmonic currents of utility and customer side. Z_c and Z_u represent the equivalent harmonic

FIGURE 1 Equivalent circuit for harmonic emission level estimation



impedance of utility and customer side, respectively. When \dot{I}_u and \dot{I}_c work alone, the harmonic contribution of customer side and utility side at PCC is:

$$\begin{cases} \dot{U}_{\text{pcc-c-real}} = \frac{Z_c Z_u}{Z_c + Z_u} \left(\frac{\dot{U}_{\text{pcc}}}{Z_c} + \dot{I}_{\text{pcc}} \right), \\ \dot{U}_{\text{pcc-u}} = \dot{U}_{\text{pcc}} - \dot{U}_{\text{pcc-c}} \end{cases} \quad (2)$$

where $\dot{U}_{\text{pcc-c-real}}$ and $\dot{U}_{\text{pcc-u}}$ represent harmonic emission levels of the customer and utility side when both Z_u and Z_c are considered, independently. Existing evaluation methods based on the assumption that $|Z_u| \ll |Z_c|$, thus, Z_c can be omitted, and Equation (2) can be rewritten as:

$$\begin{cases} \dot{U}_{\text{pcc-c-appro}} = Z_u \dot{I}_{\text{pcc}} \\ \dot{U}_{\text{pcc-u}} = \dot{U}_{\text{pcc}} - \dot{U}_{\text{pcc-c}} \end{cases}, \quad (3)$$

where $\dot{U}_{\text{pcc-c-appro}}$ represents the approximate value of the customer side harmonic emission level when Z_c is omitted. According to Equation (3), the critical parameter for harmonic emission level estimation is Z_u . Therefore, lots of previous works focus on the calculation of utility side harmonic impedance, which requires the parameters of the system side cannot change, that is, I_u and Z_u must be constant, during the measurement period.

2.2 | Harmonic emission level estimated error of traditional method

Customer side harmonic impedance is often omitted in the published works^{11-13,16,18,20,21} when estimating the harmonic emission level. Because in traditional industrial systems, the customer side harmonic impedance is usually much large than the utility side. When this condition meets, the effect of Z_c can be omitted when estimating its harmonic contribution. However, with the electronic equipment connecting to the power system using LCL/LC filters, it decreases the customer side harmonic impedance and makes the harmonic impedance of both sides nearly equal in some harmonic orders. If we want to calculate the harmonic contribution of each side accurately, the customer side harmonic impedance cannot be ignored anymore. To quantify the effect of Z_c on the harmonic contribution assessment, we illustrate the relative errors of customer side harmonic emission level as shown in Equation (4) by Equations (2) and (3).

$$\begin{aligned} \delta_{U_{\text{pcc-c}}} &= \left(\left| \dot{U}_{\text{pcc-c-real}} - \dot{U}_{\text{pcc-c-appro}} \right| \right) / \left| \dot{U}_{\text{pcc-c-real}} \right| = \\ &\left(\left| \frac{Z_c Z_u}{Z_c + Z_u} \left(\frac{\dot{U}_{\text{pcc}}}{Z_c} + \dot{I}_{\text{pcc}} \right) \right| - \left| Z_u \dot{I}_{\text{pcc}} \right| \right) / \left| \frac{Z_c Z_u}{Z_c + Z_u} \left(\frac{\dot{U}_{\text{pcc}}}{Z_c} + \dot{I}_{\text{pcc}} \right) \right| \leq \\ &\left| \frac{Z_c Z_u}{Z_c + Z_u} \left(\frac{\dot{U}_{\text{pcc}}}{Z_c} + \dot{I}_{\text{pcc}} \right) - Z_u \dot{I}_{\text{pcc}} \right| / \left| \frac{Z_c Z_u}{Z_c + Z_u} \left(\frac{\dot{U}_{\text{pcc}}}{Z_c} + \dot{I}_{\text{pcc}} \right) \right| = \left| \frac{\dot{U}_{\text{pcc}} - Z_u \dot{I}_{\text{pcc}}}{\dot{U}_{\text{pcc}} + Z_c \dot{I}_{\text{pcc}}} \right|, \end{aligned} \quad (4)$$

and \dot{I}_{pcc} shown in Equation (1), $\delta_{U_{\text{pcc}-c}}$ in Equation (4) can be represented as:

$$\delta_{U_{\text{pcc}-c}} \leq \left| \frac{\dot{U}_{\text{pcc}} - Z_u \dot{I}_{\text{pcc}}}{\dot{U}_{\text{pcc}} + Z_c \dot{I}_{\text{pcc}}} \right| = \left| \frac{\frac{Z_c Z_u}{Z_c + Z_u} (\dot{I}_u + \dot{I}_c) - Z_u \left(\frac{Z_c}{Z_c + Z_u} \dot{I}_c - \frac{Z_u}{Z_c + Z_u} \dot{I}_u \right)}{\frac{Z_c Z_u}{Z_c + Z_u} (\dot{I}_u + \dot{I}_c) + Z_c \left(\frac{Z_c}{Z_c + Z_u} \dot{I}_c - \frac{Z_u}{Z_c + Z_u} \dot{I}_u \right)} \right| = \left| \frac{|\dot{I}_u|}{|\dot{I}_c|} \right| / \left| \frac{Z_c}{Z_u} \right|. \quad (5)$$

The estimated error is associated with the harmonic impedance amplitude ratio $|Z_c|/|Z_u|$ and the harmonic source amplitude ratio $|\dot{I}_u|/|\dot{I}_c|$. When $|\dot{I}_u|/|\dot{I}_c|$ keeps constant, the bigger the value of $|Z_c|/|Z_u|$, the smaller the estimated error of customer side harmonic emission level. When $|Z_u| < < |Z_c|$, the estimation error is approximate zero. Yet, when filters are installed on the customer side, it is hard to establish its basic assumption that the harmonic impedance of the customer side is much larger than that of the utility side. Thus, a big estimated error will be caused if only the utility side harmonic impedance Z_u is used to calculate the customer harmonic emission level. In this condition, both Z_u and Z_c should be considered, and a method can calculate the harmonic impedances of both sides should be developed.

3 | PROPOSED METHOD

ICA is a statistical signal processing technique to recover the latent variables or source signals that are mixed by an unknown matrix. It can be extended for the separation of complex-valued signals, which facilitates the power system analysis in the frequency domain. To use ICA solve impedance estimation problem, some requirements for the original and measured signals need to be satisfied: (a) the number of measured signals M is greater or equal to the number of original signals N; (b) at most, one of the original signals is Gaussian distributed; and (c) the original signals are statistically independent. In this problem, the first condition is always satisfied, as the number of measured signals is equal to the number of source signals. As for the second and third conditions, the harmonic voltages and currents measured at PCC can be decomposed into the fast- and slow-varying components by utilizing a moving average filter. The fast-varying components are independent and usually have non-Gaussian distributed.¹⁹ Therefore, the moving average filter should be applied to extract the fast-varying components of measured harmonic voltages and currents. Then, ComplexICA can be used to separate the harmonic sources and calculate the harmonic impedances of both sides.

3.1 | Traditional ComplexICA method

Generally speaking, the critical point to estimate the ICA model is non-Gaussianity. According to the Lindeberg-Feller Central Limit Theory,²⁴ the distribution of a sum of independent random variables tends toward a Gaussian distribution. Therefore, a sum of two independent random variables usually has a distribution that is closer to Gaussian than any of the two original random variables. ComplexICA obtains the recovered signals by maximizing the non-Gaussianities of the separated signals; an important measure of non-Gaussianity is given by negentropy.

$$J(x) \approx [E\{G(x)\} - E\{G(v)\}]^2, \quad (6)$$

where random variable x and v are of zero mean and unit variance. And v is accorded with Gaussian distribution. Function G is non-quadratic function, which can be chosen as:

$$G(u) = -\exp(-u^2/2). \quad (7)$$

Then, the ComplexICA model can be expressed as:

$$X = AS, \quad (8)$$

where $X = \begin{bmatrix} \dot{U}_{\text{pcc-fast}}; \dot{I}_{\text{pcc-fast}} \end{bmatrix}$ are the fast-varying components of harmonic voltages and currents measured at PCC. $S = \begin{bmatrix} \dot{I}_{\text{u-fast}}; \dot{I}_{\text{c-fast}} \end{bmatrix}$ are the fast-varying components of utility and customer side harmonic current source. Matrix A is unknown and mixed with Z_u and Z_c .

To solve Equation (8), X is preprocessing by centering and whitening. The ICA is used to estimate the separating matrix H , and the separating matrix H can then be used to recover source signals as shown in the following equation:

$$S^* = HX, \quad (9)$$

where $S^* = \begin{bmatrix} \dot{I}_{\text{u-fast}}^* \\ \dot{I}_{\text{c-fast}}^* \end{bmatrix}$, $H = \begin{bmatrix} h_{11} & h_{12} \\ h_{21} & h_{22} \end{bmatrix}$. S^* is the matrix of estimated source signals. H is the estimated mixing matrix. The results of ICA have scaling indeterminacy, therefore, assuming that the estimated source signals and the real source signals accord with Equation (10):

$$\begin{bmatrix} \dot{I}_{\text{u-fast}}^* \\ \dot{I}_{\text{c-fast}}^* \end{bmatrix} = \begin{bmatrix} k_u \dot{I}_{\text{u-fast}} \\ k_c \dot{I}_{\text{c-fast}} \end{bmatrix}. \quad (10)$$

Submitting Equation (10) in Equation (9), then:

$$\begin{bmatrix} \dot{I}_{\text{u-fast}} \\ \dot{I}_{\text{c-fast}} \end{bmatrix} = \begin{bmatrix} \frac{h_{11}}{k_u} & \frac{h_{12}}{k_u} \\ \frac{h_{21}}{k_c} & \frac{h_{22}}{k_c} \end{bmatrix} \begin{bmatrix} U_{\text{pcc-fast}} \\ I_{\text{pcc-fast}} \end{bmatrix}. \quad (11)$$

From Equation (1), we have:

$$\begin{bmatrix} \dot{I}_u \\ \dot{I}_c \end{bmatrix} = \begin{bmatrix} \dot{I}_{\text{u-slow}} + \dot{I}_{\text{u-fast}} \\ \dot{I}_{\text{c-slow}} + \dot{I}_{\text{c-fast}} \end{bmatrix} = \begin{bmatrix} \frac{1}{Z_u} & 1 \\ \frac{1}{Z_c} & -1 \end{bmatrix} \begin{bmatrix} \dot{U}_{\text{pcc}} \\ \dot{I}_{\text{pcc}} \end{bmatrix}. \quad (12)$$

The average moving filter is a kind of linear filter. Thus, it does not change the mixing matrix. Then, we can calculate harmonic impedance by comparing Equations (11) and (12), and the results are shown in the following equation:

$$\begin{cases} Z_1 = h_{12}/h_{11} \\ Z_2 = h_{22}/h_{21} \end{cases}. \quad (13)$$

As analyzed before, the estimated error is closely related to the amplitude ratio between utility harmonic impedance and customer harmonic impedance. Under some frequency, if Z_u is far smaller than Z_c , only Z_u is needed during the process of harmonic emission level estimation. On the contrary, if the value of Z_u is close to Z_c , it is critical to calculating both Z_u and Z_c to ensure accuracy. There is a simple criterion to judge whether Z_u is far smaller than Z_c or not. From Equation (1), if $Z_u < < Z_c$, we have:

$$\dot{I}_{\text{pcc}} \approx \dot{I}_c. \quad (14)$$

Thus, if the pattern of \dot{I}_c is highly accorded with \dot{I}_{pcc} , $Z_u < < Z_c$ meets, otherwise, the value of Z_u is close to Z_c .

The estimated results have high accuracy if the separated signals obtained using ComplexICA are similar to the true signals. The amount of data is relevant to its statistical characteristics capture. Therefore, the accuracy of this algorithm is related to the amount of data for each calculation. One way to get enough data for calculation is to increase the sampling time at the risk of harmonic impedance change. However, in the ComplexICA model, the mixed matrix is combined by the harmonic impedance, which requires that harmonic impedances of both sides are roughly constant during

the calculation period. Reducing the amount of data can guarantee constant impedances. Yet, the lack of statistical characteristics of the data still results in an estimated error. Furthermore, local convergence and optimum properties of ComplexICA also have a great effect on the impedance estimation. Therefore, an improved method should be proposed to enhance the separation capability of ComplexICA when little data are involved in the calculation. Besides, some additional conditions should consider improving the performance of the algorithm to avoid local convergence.

3.2 | Proposed method

The constrained independent component analysis first proposed in Ref.²⁵ In this paper, the author solves the indeterminacy problems in the ICA algorithm. The principle of constrained independent component analysis is adding the additional requirement or the available prior information of the original source signals or the mixing matrix into the ICA in the form of equality or inequality constraints. Then, the separated signals, which coincide closely with the true original signal, will be obtained.

If some prior information of the impedance matrix or harmonic sources can be found, the estimation accuracy will increase. In some paper, the measured harmonic voltages and currents at PCC when the load is shutdown are selected as the prior information of the utility side harmonic sources,²³ which requires the utility harmonic source to keep steady during the whole calculation period. However, the utility harmonic sources are usually composed of the harmonic sources except for the concerned nonlinear loads, so it varies with these harmonic sources. In the multi-wind farm, the utility side contains other wind farm harmonic sources, which lead to the instability of the utility side harmonic sources.²² Besides, the filters installed on the wind farm side result in the decrease of the customer side harmonic impedance. In this case, the accuracy of harmonic contributions evaluation can be improved only that both utility and customer side harmonic impedances are estimated. However, no prior information on the customer side is provided. Therefore, a new constraint condition should be offered.

According to Equation (12), the separated signals of ComplexICA are the fast-varying components of utility and customer side harmonic sources, and the separated matrix is the harmonic admittance matrix for the concerned harmonic order. It indicates that the second column of the separated matrix should be 1 or -1, which means the elements in the second column of the separated matrix obtained by the ComplexICA are real numbers when the source signals are recovered accurately. It can be expressed as:

$$\begin{cases} \text{imag}(h^*(1,2)) \approx 0 \\ \text{imag}(h^*(2,2)) \approx 0 \end{cases}. \quad (15)$$

The recovered signals only have the amplitude scaling and no phase deviation in this condition. Based on Equations (10)-(12), we have:

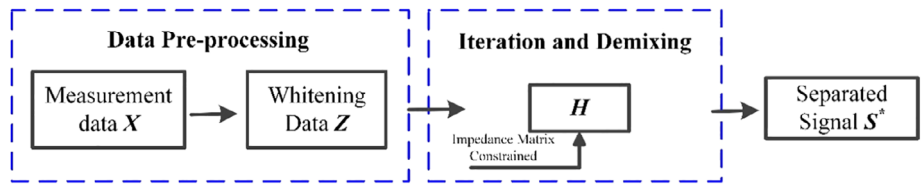
$$\begin{bmatrix} \dot{I}_{1-\text{fast}}/h_{12} \\ \dot{I}_{2-\text{fast}}/h_{22} \end{bmatrix} = \begin{bmatrix} h_{11}/h_{12} & 1 \\ h_{21}/h_{22} & 1 \end{bmatrix} \cdot \begin{bmatrix} \dot{U}_{\text{pcc-fast}} \\ \dot{I}_{\text{pcc-fast}} \end{bmatrix}. \quad (16)$$

From Equation (16), if there is phase derivation between recovered signals and original source signals depends on h_{12} and h_{22} . If the imaginary part of the h_{12} and h_{22} approach to zero, there is only the amplitude scaling of the recovered signals. Conversely, the recovered signals have not only amplitude scaling but also phase offset compared with the original source signals.

The key point of harmonic impedance estimation is making the recovered signal highly similar to the original source signals. The principle of ComplexICA is finding the signals with maximizing non-Gaussianity. Thus, inadequate optimization arises when the non-Gaussianity of mixed signals are weaker than the original signals. In the proposed method, Equation (15) is considered as a constrained condition for constrained ComplexICA, the recovered signals and separated matrix are selected when the imaginary part of the second column of the separated matrix approaches to zero. Figure 2 is the principle diagram of constrained ICA based on impedance matrix constrained.

The results utilizing constrained ComplexICA are:

FIGURE 2 Principle diagram of the constrained ICA based on impedance matrix



$$S^* = H^* \cdot \begin{bmatrix} \dot{U}_{\text{pcc-fast}} \\ \dot{I}_{\text{pcc-fast}} \end{bmatrix} = \begin{bmatrix} h_{11}^* & h_{12}^* \\ h_{21}^* & h_{22}^* \end{bmatrix} \cdot \begin{bmatrix} \dot{U}_{\text{pcc-fast}} \\ \dot{I}_{\text{pcc-fast}} \end{bmatrix}, \quad (17)$$

where \tilde{S}^* is the recovered signals. H^* is separated matrix and can be expressed as:

$$H^* = \begin{bmatrix} h_{11}^* & h_{12}^* \\ h_{21}^* & h_{22}^* \end{bmatrix} = \begin{bmatrix} a_{11} + jb_{11} & a_{12} + j0 \\ a_{21} + jb_{21} & a_{22} + j0 \end{bmatrix}$$

Then, as method based on ComplexICA, the harmonic impedance of utility side and customer side can be calculated using Equation (18):

$$\begin{cases} Z_1 = h_{12}^*/h_{11}^* \\ Z_2 = h_{22}^*/h_{21}^* \end{cases}. \quad (18)$$

The results of proposed method also have ordering indeterminacy, which means it is not clear whether $S^* = \begin{bmatrix} i_{u\text{-fast}}^* \\ i_{c\text{-fast}}^* \end{bmatrix}$ or $S^* = \begin{bmatrix} i_{c\text{-fast}}^* \\ i_{u\text{-fast}}^* \end{bmatrix}$. Because the real part of impedance represents resistive part, it is always positive; we can solve this problem according to following equation:

$$Z_i = \begin{cases} Z_s, & \text{real}(Z_i) > 0 \\ -Z_c, & \text{real}(Z_i) < 0 \end{cases}, i=1,2. \quad (19)$$

Then, the proposed harmonic impedance estimation method based on the impedance matrix constrained is completed. And the flow diagram of proposed method is shown in Figure 3.

4 | CASE STUDY

4.1 | Simulation case and algorithm analysis

The circuit model shown in Figure 1 is simulated in Matlab/Simulink to compare the performance of different harmonic impedance estimation methods. Then, 10 000 harmonic voltages and currents data at PCC are generated randomly according to Equation (1). The case study is used to verify the performance of the proposed method, and the analysis results are suitable for any other harmonics. Then, the 10 000 data are divided into 100 segments for simulation.

4.1.1 | Parameter setting of case study

It is definite that all existing methods can provide accurate results when the utility side is ideal and the harmonic impedance of the customer side is much larger than that of the utility side. The focus of the simulation verification is thus to study the impact of system variation and the different harmonic impedance ratios on different methods. The specific parameters of the harmonic sources and the harmonic impedance are set as shown in Table 1.

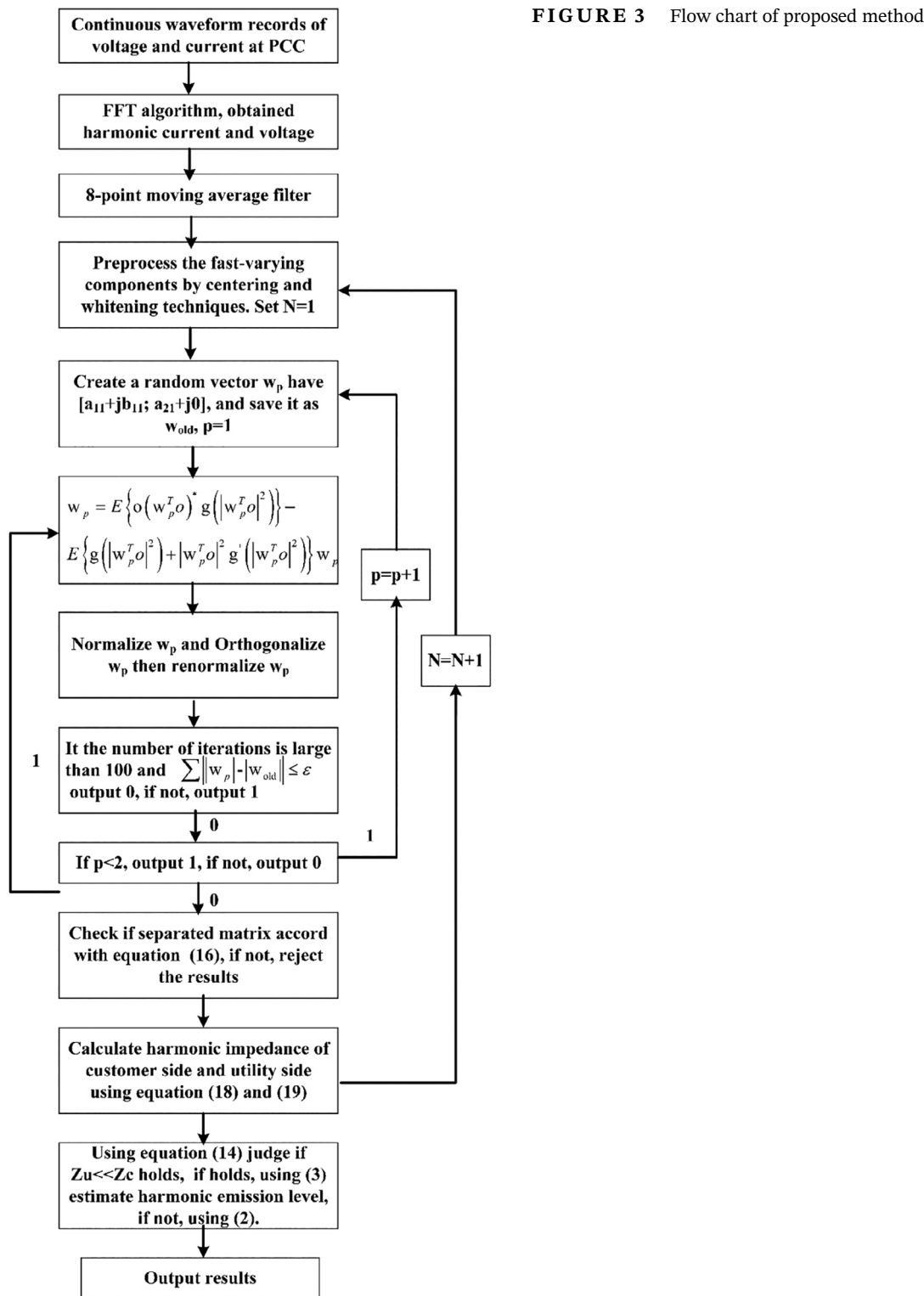


FIGURE 3 Flow chart of proposed method

4.1.2 | Customer harmonic emission level estimated error for different $|Z_c|/|Z_u|$

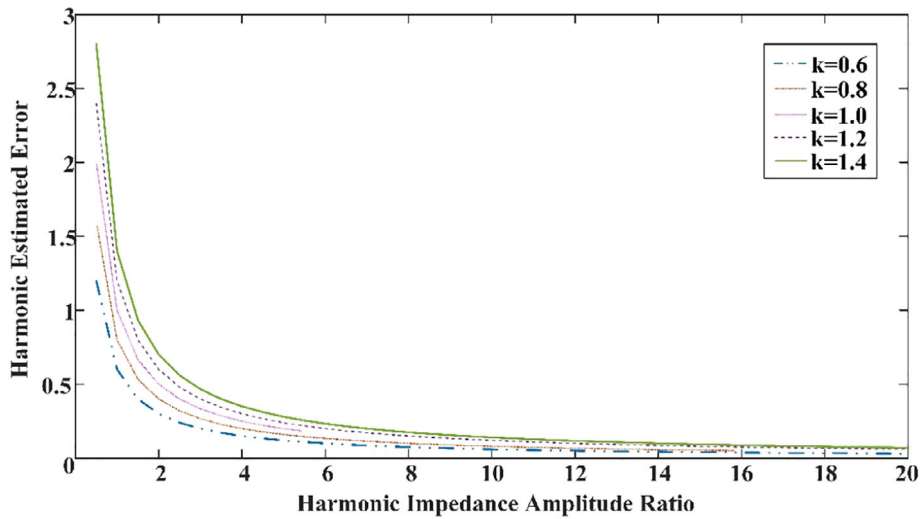
In most of the existing methods, the customer side harmonic impedance is omitted during the process of harmonic contribution evaluation. As the analysis in Section 2.2, we find that the customer's harmonic emission level-estimated errors are related to the harmonic impedance amplitude ratio and the harmonic source amplitude ratio. To better indicate the influence of the harmonic impedance amplitude ratio on the harmonic emission level-estimated error, we can obtain the estimated error curve in accordance with Equation (5) as shown in Figure 4.

TABLE 1 Parameter setting in the simulation study

Variable	Magnitude		phase angle	
	Mean value	Variation	Mean value	Variation
\dot{I}_c	40A	Sine fluctuation: $\pm 10\%$ Random disturbance: $\pm 5\%$	60°	Sine fluctuation: $\pm 10\%$ Random disturbance: $\pm 5\%$
\dot{I}_u	$k \cdot \dot{I}_c$	Sine fluctuation: $\pm 10\%$ Random disturbance: $\pm 5\%$	30°	Sine fluctuation: $\pm 10\%$ Random disturbance: $\pm 5\%$
Z_u	10.44 Ω	Random disturbance: $\pm 5\%$	73.3°	Random disturbance: $\pm 5\%$
Z_c	17.89 Ω	Random disturbance: $\pm 5\%$	63.4°	Random disturbance: $\pm 5\%$
	101.12 Ω	Random disturbance: $\pm 5\%$	81.5°	Random disturbance: $\pm 5\%$

Note: Where: $k = 0.2, 0.4, \dots, 1.6, 1.8$ separately. $Z_u = (3 + j10)\Omega$, $Z_c = (8 + j16)\Omega$ and $Z_c = (15 + j100)\Omega$.

FIGURE 4 Errors of customer harmonic emission level estimation at different $|Z_c|/|Z_u|$. A, utility side harmonic impedance when $Z_c = (8 + j16)\Omega$. B, Customer side harmonic impedance when $Z_c = (8 + j16)\Omega$. C, Customer side harmonic impedance when $Z_c = (15 + j100)\Omega$

**TABLE 2** Estimated errors of customer harmonic emission level

Customer side harmonic emission level-estimated errors (%)												
	$p = 0.5$	$p = 1$	$p = 2$	$p = 4$	$p = 6$	$p = 8$	$p = 10$	$p = 12$	$p = 14$	$p = 16$	$p = 18$	$p = 20$
$k = 0.6$	120	60	30	15	10	7.5	6	5	4.28	3.75	3.33	3
$k = 0.8$	160	80	40	20	13.3	10	8	6.7	5.7	5	4.4	4
$k = 1.0$	200	100	50	25	16.7	12.5	10	8.3	7.1	6.25	5.5	5
$k = 1.2$	240	120	60	30	20	15	12	10	8.6	7.5	6.7	6
$k = 1.4$	280	140	70	35	23.3	17.5	14	11.7	10	8.75	7.8	7

Note: Where: $p = |Z_c|/|Z_u|$.

From Figure 4, the estimated error of customer harmonic emission level decreases with the increase of $|Z_c|/|Z_u|$ when the amplitude ratio of harmonic source, which is represented by k in this case, keeps constant. Table 2 demonstrates the relationship between harmonic estimated error and the value of $|Z_c|/|Z_u|$.

It is apparent that the estimated errors are small when the customer side harmonic impedance is much large than that of the utility side, that is, $|Z_c|$ is 10 times larger than $|Z_u|$. In this case, Z_c can be omitted, and the harmonic emission level can be calculated utilizing Equation (3) approximately, which is often adopted for harmonic contribution evaluation of the traditional industrial nonlinear loads, such as arc furnace. On the contrary, the estimated error is not acceptable when the amplitude of Z_u is close to that of Z_c , and the harmonic emission levels should be calculated using Equation (2). With more and more power electronic equipment connected to the power system, the LCL/LC filters

installed on the customer side can potentially make the assumption that $|Z_u| < |Z_c|$ invalid for some harmonic orders. Most of the previous works are based on the assumption that $|Z_u| < |Z_c|$, and focus on the estimation of utility side harmonic impedance, which is not suitable for the new case. Thus, both Z_u and Z_c should be provided to obtain a more reliable harmonic emission level assessment result in the renewable energy system, and a method can calculate both sides' harmonic impedance should be developed.

4.1.3 | Harmonic impedance estimated error for different methods

In this section, four typical harmonic impedance estimation methods: (a) binary linear regressive method; (b) method based on covariance characteristic of random vectors; (c) ComplexICA method; and (d) proposed constrained ICA method are used to calculate harmonic impedance. The relative errors of the real and imaginary parts of harmonic impedance are obtained separately using Equation (20).

$$\text{error\%} = \frac{1}{n} \sum_{i=1}^n \left| \frac{Z_{i,\text{calculated}} - Z_{\text{true}}}{Z_{\text{true}}} \right| * 100\%, \quad (20)$$

where $Z_{i,\text{calculated}}$ is the estimated harmonic impedance for the i th time interval. Z_{true} is the actual value of the harmonic impedance. Background harmonic is a critical factor affecting the performance of harmonic impedance estimation. In this paper, we set k varies from 0.2 to 1.8 in steps of 0.2. Then, four harmonic impedance methods aforementioned are adopted for calculating harmonic impedance and all the results, and the errors for the real and imaginary parts of the utility side harmonic impedance are shown in Tables 3 and 4, respectively.

When $Z_c = (8 + j16)\Omega$, $|Z_c|$ is close to $|Z_u|$. Based on the estimation errors presented in Table 3, it is obvious that the estimation errors of method 4 are relatively low and change slowly with the increase of the background harmonic (ie, the increase of k). Yet, the calculation errors of methods 1 and 2 are relatively large. Although the results of method 3 are smaller than those of methods 1 and 2, it has not only larger errors but also bigger fluctuations than method 4.

When the customer side harmonic impedance is set to $(15 + j100)\Omega$, $|Z_c|$ is much larger than $|Z_u|$. The calculation results of each method are shown in Table 4. By the results, the estimation errors of the real part and imaginary part of utility side harmonic impedance become large with the increase of background harmonic for methods 1 and 2 because these two methods are sensitive to the background harmonic fluctuation. On the contrary, methods 3 and 4 show better performance. Evidently, the calculation errors of method 4 are smaller and more stable than those of method 3 with the change of background harmonic.

To make the estimation errors visualized, the relative errors of utility side harmonic impedance when $Z_c = (8 + j16)\Omega$ and $Z_c = (15 + j100)\Omega$ are shown in Figure 5A,C, respectively. When $Z_c = (8 + j16)\Omega$, the amplitude of Z_c is approximately equal to that of Z_u , therefore, the estimation errors of customer side harmonic impedance for methods

TABLE 3 Errors (%) of utility harmonic impedance $Z_c = (8 + j16)\Omega$

<i>k</i>	Method 1		Method 2		Method 3		Method 4	
	Real (Z_u)	Imag (Z_u)						
0.2	39.71	88.95	4.14	5.92	3.67	3.86	3.45	2.38
0.4	41.33	84.05	10.01	8.47	3.94	4.95	3.68	4.35
0.6	52.62	79.21	21.56	14.36	5.68	8.69	5.15	8.34
0.8	102.11	82.16	31.11	21.44	9.56	9.55	3.67	3.93
1.0	95.45	75.49	38.57	28.59	15.46	12.67	2.82	3.72
1.2	128.79	69.18	53.22	36.83	9.42	11.38	3.64	6.53
1.4	146.64	73.34	57.47	48.05	9.17	15.63	3.94	6.85
1.6	170.23	70.89	76.37	57.83	9.51	17.06	5.89	7.88
1.8	182.37	72.12	94.23	78.26	16.19	18.24	7.44	8.05

TABLE 4 Errors (%) of utility harmonic impedance $Z_c = (15 + j100)\Omega$

k	Method 1		Method 2		Method 3		Method 4	
	Real (Z_u)	Imag (Z_u)						
0.2	10.34	8.53	3.57	5.46	4.55	4.23	1.13	1.34
0.4	17.23	15.19	6.79	7.45	4.67	4.19	2.05	2.77
0.6	33.47	36.35	10.34	11.89	7.98	9.34	4.35	6.16
0.8	45.79	39.38	15.89	20.57	10.15	12.78	6.66	6.59
1.0	60.42	55.87	27.89	25.77	11.79	16.83	4.89	3.76
1.2	80.63	84.55	37.73	33.49	9.47	14.25	5.43	6.34
1.4	110.32	91.36	50.84	45.77	8.53	15.13	4.83	5.92
1.6	145.14	104.61	69.82	62.43	13.22	9.78	8.37	8.43
1.8	132.67	94.67	79.37	75.55	7.34	10.47	5.96	7.04

3 and 4 are shown in Figure 5B. Because when the harmonic impedance amplitude of both sides is close, customer side harmonic impedance is also essential when calculating the harmonic emission level. By comparison, the accuracy of methods 1 and 2 is low. Besides, these errors grow sharply with the increase of background harmonic. For method 1, the binary regressive method requires that the background harmonic keep stable, and the multiple correlation characteristics can also cause the wrong result. As for method 2, when the precondition that $Z_u < Z_c$ holds, the harmonic currents at PCC are mainly determined by I_c , which means I_u and I_{pcc} are approximately independent. Thus, method 2 is invalid when Z_u approaches Z_c . Compared with methods 1 and 2, the results of ComplexICA are improved but not vintage, the lack of data for each calculation has a negative effect on impedance estimation. What's more, it is hard to calculate both Z_u and Z_c when the amplitude of Z_u and Z_c is close to each other. On the contrary, the proposed method can calculate the harmonic impedance of both sides correctly by utilizing the essential feature of the impedance matrix.

4.1.4 | Error analysis for ComplexICA method

As mentioned before, the amount of sample data may affect the accuracy of the results of ComplexICA. If there are little data involved in the calculation, every run will have different results. It is widely accepted that if enough data are used to calculate, a reliable result can be obtained. However, more data mean more measurement time, and more measurement time means more risk of the impedance change. In this part, we mainly discuss the impact of sample data.

The optimization objective of complexICA is the maximization of non-Gaussianity, and the non-Gaussianity is measured by negative entropy. According to the definition of entropy, the probability density function is an important parameter to calculate the entropy. As is known to all, it is easier to capture the statistical characteristic of the sample data when the sample size is large. Therefore, the number of sample data has a great influence on the estimation of the probability density function of these data, which is related tightly to the calculation of negative entropy. Moreover, lack of data may result in local convergence or divergence, which can also cause wrong results. By running ComplexICA repeatedly under $k = 1$ using sample data with different sizes, the harmonic impedance estimation errors are obtained shown in Figure 6.

As is shown in Figure 6, the calculation results are not stable when the number of sample data is low. Every run can get different results, and the errors among these results have a big difference. With the increasing of sample data, the running results become stable, and the estimation error decreases.

4.2 | Field case verification

4.2.1 | Field case 1

Case description

A multi-wind farm system (shown in Figure 7) is used to compare the performance of each method, and the parameter for the tested wind farm is shown in Table 5. The voltages and currents are recorded on the 110 kV

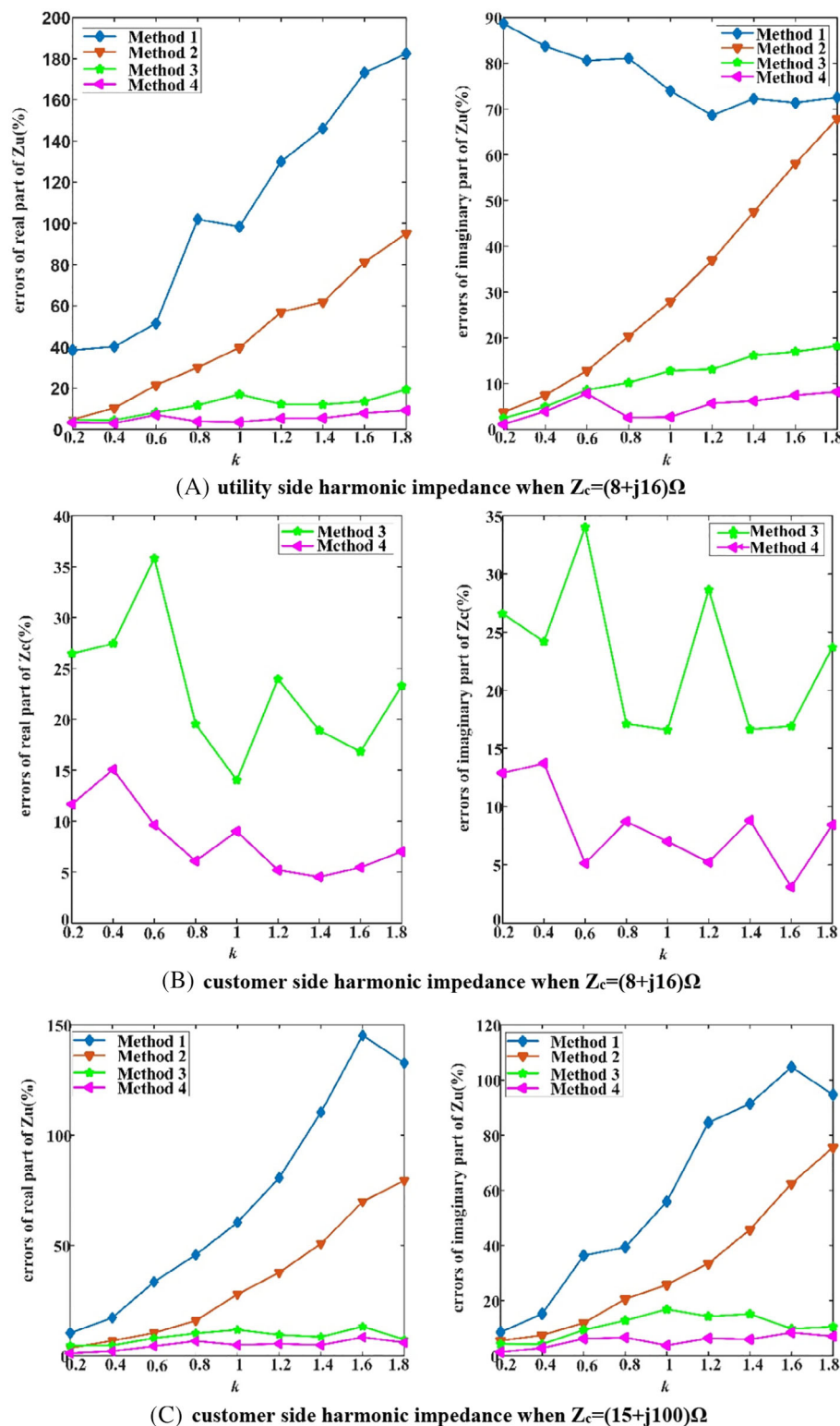
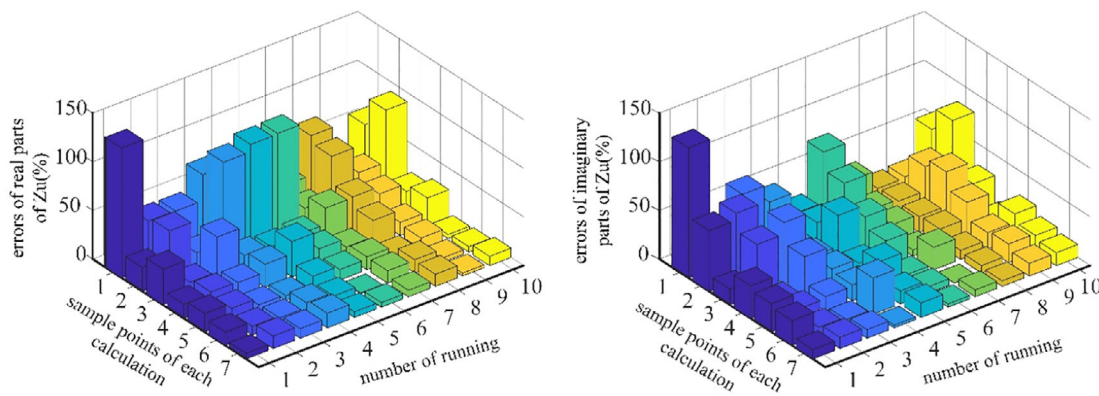


FIGURE 5 Errors of real and imaginary parts of Z_u and Z_c

grid connection point of the test wind farm, and the sampling frequency is set at 10 kHz, which can ensure the statistical characteristics of recorded data and avoid increasing the risk of amplifying the random noise simultaneously.

All the harmonic data are obtained utilizing the fast Fourier transformation. It is widely accepted that the fundamental frequency deviation may result in harmonic phase angle variation during the process of the fast Fourier transformation, which may result in an estimation error of harmonic impedance. Because the phase change of fundamental



sample points of each calculation:

- 1: 100 sample points for each calculation; 2: 500 sample points for each calculation
- 3: 1000 sample points for each calculation; 4: 3000 sample points for each calculation
- 5: 6000 sample points for each calculation; 6: 9000 sample points for each calculation
- 7: 10000 sample points for each calculation.

FIGURE 6 Errors comparison of ComplexICA

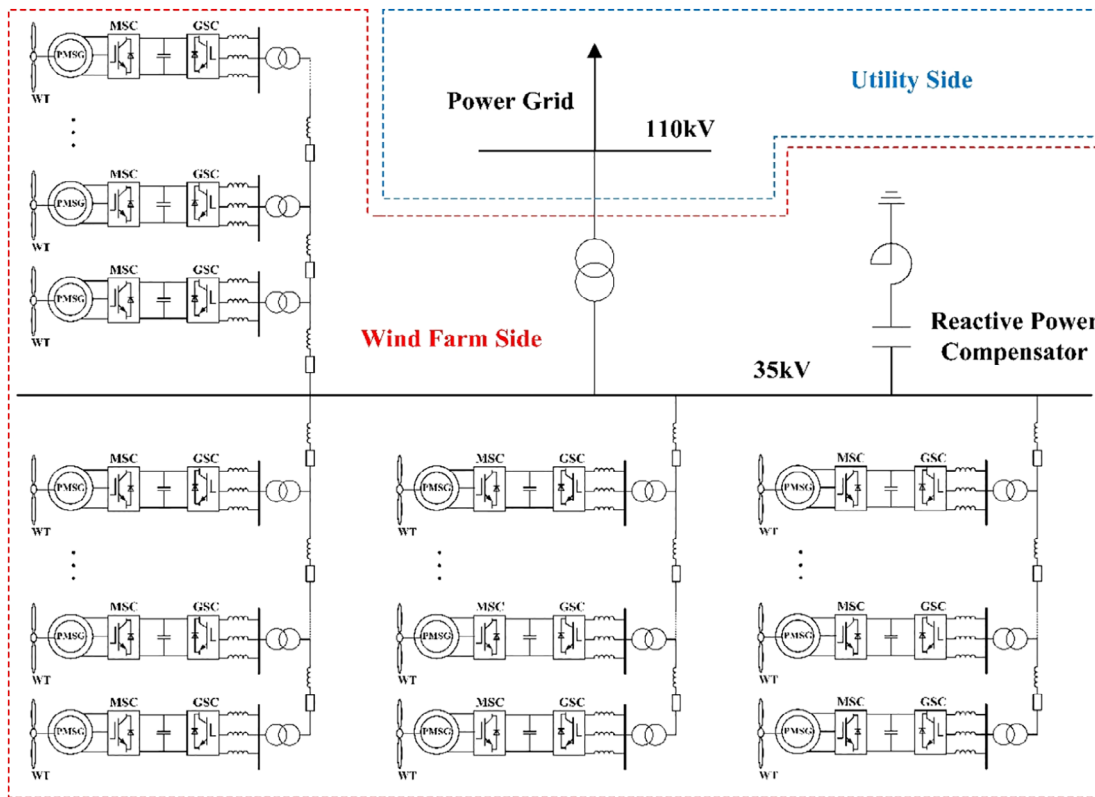


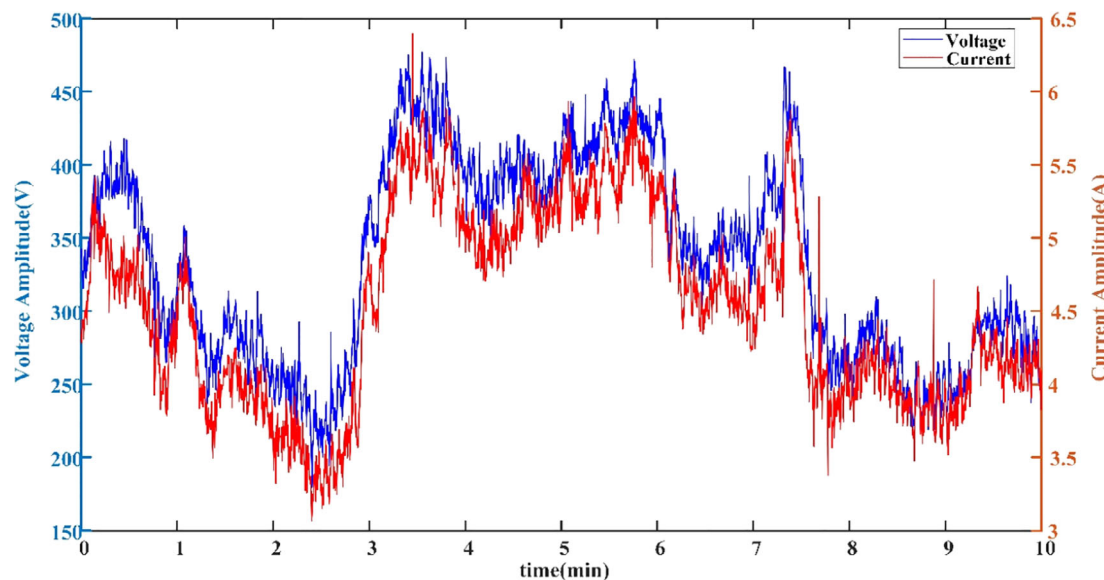
FIGURE 7 Topological structure of tested multi-wind farms system

voltage is small, all the harmonic phases in this paper are referenced to the fundamental voltage; the phase errors caused by fundamental frequency deviation can be eliminated in this way.

From the recorded data, the ratio of 5th harmonic is relatively high. Thus, the 5th harmonic is taken for an example for analysis. The 5th harmonic voltage and current data for 10 minutes are shown in Figure 8, and there are five data points per second. In practice, Z_u changes slowly and is usually stable within a short-time segment.^{11,12,21} Yet, the fluctuations of Z_c are relatively frequent. It is presented in Ref.²¹ that the weaker the fluctuation of fundamental current, the less the variation of Z_c . During the measured period, the fundamental current fluctuates weakly, thus, the harmonic impedances are relatively stable to some degree. However, there is still a risk of the change of variation for such a long

TABLE 5 Parameter of the tested wind farm

Parameter	Value
PCC	Rated voltage: 110 kV, Short circuit impedance: $(3 + j12.45) \Omega$
Installed capacity	49.5 MW
Collecting feeder	Feeder 1: wind turbine 2-8, 21, 11.13 km, $(0.191 + j0.357) \Omega/\text{km}$ Feeder 2: wind turbine 16-20, 22, 9.96 km, $(0.191 + j0.357) \Omega/\text{km}$ Feeder 3: wind turbine 11-14, 23, 4.14 km, $(0.191 + j0.357) \Omega/\text{km}$ Feeder 4: wind turbine 1, 9, 15, 24, 25, 3.35 km, $(0.191 + j0.357) \Omega/\text{km}$
Wind turbine transformer	Transformer ratio: 0.69/37 kV, Rated capacity: 2.35MVA
FC	Rated capacity: 12MVar, Rated Voltage: 35 kV

**FIGURE 8** The 5th harmonic voltages and currents at PCC

period. To solve this problem, the PCC data are equally divided into 10 segments to further keep the harmonic impedance keep constant in a single calculation interval. Consequently, it can be considered that harmonic impedance can keep stable in a short period of 1 minute.

Calculation results analysis

According to the field data shown in Figure 8, the 5th harmonic impedance is calculated by using each method. The calculation results are shown in Figure 9.

During such a short period of the power system, the fluctuation of utility side impedance is usually small. As can be seen from Figure 9, the calculation results of methods 1, 2, and 3 fluctuate acutely, which do not accord with actual conditions. On the one hand, in the wind farm system, the condition that utility side harmonic impedance Z_u is far smaller than customer side harmonic impedance Z_c does not hold anymore because of the filters, which enhance the dependence between utility side harmonic current and harmonic current at PCC. Thus, the necessary condition for the covariance characteristics method is no longer valid. On the other hand, the background harmonic fluctuation may destabilize the result of binary linear regression. As for the ComplexICA method, a reliable and stable result can be obtained only when there are lots of sample data involved in each computation. Otherwise, the lack of statistical characteristics of sample data leads to the wrong result. By comparison, the results of the proposed method are more stable, which coincides with reality.

According to the rated parameter of the wind farm, we can obtain the reference harmonic impedance value of both sides. The reference value of utility side 5th harmonic impedance is calculated based on the short-circuit capacity, which is around 63.07Ω . Additionally, by using the parameter of the wind farm, we can roughly calculate

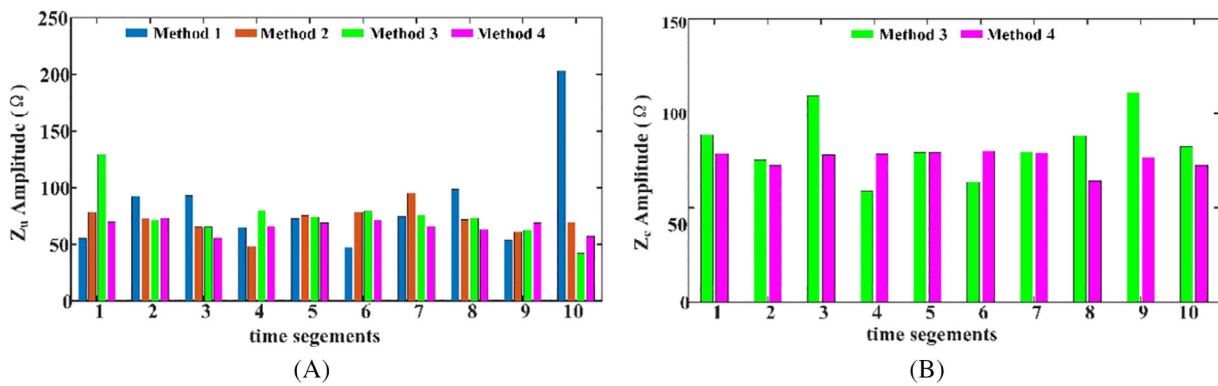
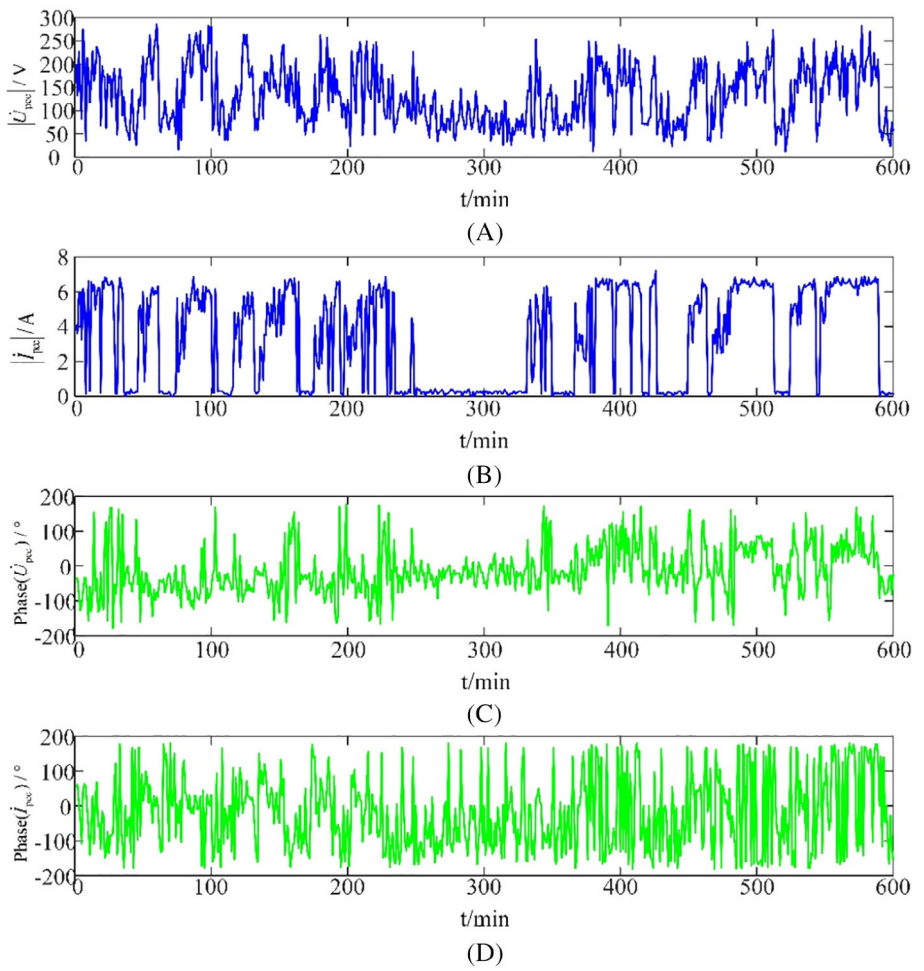


FIGURE 9 The 5th harmonic impedance estimation errors. A, Utility side, B, wind farm side

FIGURE 10 Amplitude and phase angle of the harmonic and voltage and current at PCC. A, Amplitude of 11th harmonic voltage. B, Amplitude of 11th harmonic current. C, Phase of 11th harmonic voltage. D, Phase of 11th harmonic current



the reference value of 5th harmonic impedance of wind farm side, which is around $72\ \Omega$, the harmonic impedance of both sides is close to each other, thus, both Z_u and Z_c are needed during the process of harmonic emission level estimation. Then, the harmonic impedance obtained by utilizing the proposed method by comparing average values ($|Z_u| = 65.93\ \Omega$ and $|Z_c| = 75.84\ \Omega$) with the reference values. Apparently, both Z_u and Z_c calculated by the proposed method are close to their reference values. Finally, according to the calculation results of Z_u and Z_c , the harmonic emission levels of the wind farm side and utility side at the PCC are obtained separately as $55.87\ \text{V}$ and $213.06\ \text{V}$ by utilizing Equation (2).

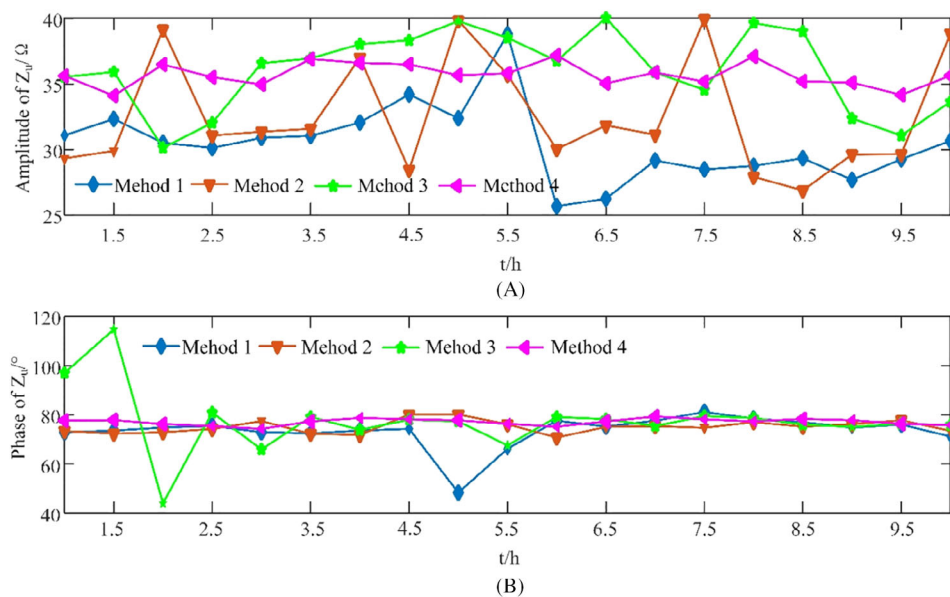


FIGURE 11 Calculation results of utility 11th harmonic impedance. A, Amplitude of 11th utility harmonic impedance, B, phase of 11th utility harmonic impedance

4.2.2 | Field case 2

The measurement data are recorded on the 150 kV busbar feeder of the 100MVA dc arc furnace in a steel plant in North China. To ensure the statistical characteristics of data, not to amplify the random noise caused by a high sampling frequency. The sampling frequency is set as 6.4 kHz, which can avoid the amplification of random noise and ensure the statistical properties of the data. All the harmonic data are obtained by utilizing the fast Fourier transformation to the sample data per minute. The variation of RMS value of magnitude and phase for the 11th harmonic voltage and current data at PCC are shown in Figure 10. To obtain more calculation data, the 600 data points are divided into 19 subintervals, that is, (1-60, 31-90, ..., 511-570, 541-600).

In this case, the customer side 11th harmonic impedance is much larger than that of the utility side, according to the analysis in Section 2.2, the harmonic emission level of the customer side and utility side can be calculated accurately only the utility side harmonic impedance is provided. Therefore, in this case, only the 11th harmonic impedance of the utility side is calculated using the aforementioned four methods, and the estimation results are shown in Figure 11. It can be seen that methods based on binary regression, the method based on random vectors covariance characteristics, and method based on ComplexICA provide lots of harmonic impedance fluctuations in this case. However, the method proposed in this paper provides more stable results that are consistent with reality. We further validate the utility harmonic impedance from the proposed method by comparing the average values, that is, 36.3Ω and 78.3° , with the corresponding reference values. During the downtime of the arc furnace, the customer devices do not work, the harmonic voltages and currents at PCC are approximately equal to the background harmonic.^{11,20} Therefore, we can calculate the reference value of the utility side harmonic impedance based on intrusive method,^{11,20} that is, 34.5Ω and 73° . Obviously, the utility harmonic impedance calculation results from the proposed method are close to the reference value.

5 | CONCLUSION

The present paper proposed an impedance matrix constrained ComplexICA-based method to estimate the harmonic emission levels at PCC. The main conclusions are as follows:

- 1 This paper proposes a harmonic impedance estimation method based on impedance matrix constraints. The inherent characteristics of the impedance matrix in the harmonic impedance estimation model are brought into the iterative process of complex ICA. It limits the separated matrix and recovers the signal that closely matches the real source signal, which achieves an accurate estimation of the harmonic impedance of both sides.
- 2 Simulation and field data verification show that the proposed method is robust to the background harmonic fluctuations. Besides, when the utility side harmonic impedance is close to the customer side, a reliable result can also be

obtained. What's more, the proposed method can reduce the calculation cycle of the harmonic impedance estimation, as it does not need a large amount of sample data for each calculation. Thus, it can decrease the risk of harmonic impedance change during the calculation process.

- 3 The proposed method can solve the problem of inaccurate calculation of customer side harmonic impedance to a certain extent compared with the previous method, but the stability of the algorithm is not ideal. How to achieve an accurate calculation of impedance on both sides needs to be further studied.

ACKNOWLEDGEMENTS

This paper was supported by the National Science Foundation of China (#51807126), the State Grid Corporation of China Research Program (SGZJDK00DWJS1900033), and China Scholarship Council.

CONFLICT OF INTEREST

The authors declare no conflict of interest.

ORCID

Xian Zheng  <https://orcid.org/0000-0002-8316-0469>

REFERENCES

1. Tentzerakis ST, Papathanassiou S. An investigation of the harmonic emissions of wind turbines. *IEEE Trans Energy Convers.* 2007;22(1):150-158.
2. Riedel P. Harmonic voltage and current transfer, and AC-and DC-side impedances of HVDC converters. *IEEE Trans Power Delivery.* 2005;20(3):2095-2099.
3. Hu H, Pan P, Song Y, He Z. A novel controlled frequency band impedance measurement approach for single-phase railway traction power system. *IEEE Trans Ind Electron.* 2019;67(1):244-253.
4. Xiao F, Ai Q. Data-driven multi-hidden-Markov model-based power quality disturbance prediction that incorporates weather conditions. *IEEE Trans Power Syst.* 2018;34(1):402-412.
5. Wang Y, Mazin HE, Xu W, Huang B. Estimating harmonic impact of individual loads using multiple linear regression analysis. *Int Trans Electr Energy.* 2016;26(4):809-824.
6. Gretsch R, Neubauer M. System impedances and background noise in the frequency range 2 kHz to 9 kHz. *Eur Trans Electr Power.* 1998;8(5):369-374.
7. Sumner M, Palethorpe B, Thomas DW, Zanchetta P, Di Piazza MC. A technique for power supply harmonic impedance estimation using a controlled voltage disturbance. *IEEE Trans Power Electron.* 2002;17(2):207-215.
8. Xu W, Ahmed EE, Zhang X, Liu X. Measurement of network harmonic impedances: practical implementation issues and their solutions. *IEEE Trans Power Delivery.* 2002;17(1):210-216.
9. Sumner M, Palethorpe B, Thomas DW. Impedance measurement for improved power quality-Part 1: the measurement technique. *IEEE Trans Power Delivery.* 2004;19(3):1442-1448.
10. Saad H, Schwob A, Vernay Y. Study of resonance issues between HVDC link and power system components using EMT simulations. Paper presented at: 2018 Power Systems Computation Conference (PSCC); June 11-15, 2018; Dublin, Ireland: IEEE.
11. Hui J, Freitas W, Vieira JC, Yang H, Liu Y. Utility harmonic impedance measurement based on data selection. *IEEE Trans Power Delivery.* 2012;27(4):2193-2202.
12. Hui J, Yang H, Lin S, Ye M. Assessing utility harmonic impedance based on the covariance characteristic of random vectors. *IEEE Trans Power Delivery.* 2010;25(3):1778-1786.
13. Yang H, Pirotte P, Robert A. Assessing the harmonic emission level from one particular customer. Paper presented at: Proceedings of the 3rd International Conference on Power Quality; 1994.
14. Huang X, Nie P, Gong H. A new assessment method of customer harmonic emission level. Paper presented at: 2010 Asia-Pacific Power and Energy Engineering Conference; March 28-31, 2010; Chengdu, China: IEEE.
15. Xu Y, Huang S, Liu Y. Partial Least-Squares Regression based harmonic emission level assessing at the point of common coupling. Paper presented at: 2006 International Conference on Power System Technology; October 22-26, 2006; Chongqing, China.
16. Langella R, Testa A. A new method for statistical assessment of the system harmonic impedance and of the background voltage distortion. Paper presented at: 2006 International Conference on Probabilistic Methods Applied to Power Systems; June 11-15, 2006; Stockholm, Sweden.
17. Mazin HE, Xu WB. Determining the harmonic impacts of multiple harmonic-producing loads. Paper presented at: 2011 IEEE Power and Energy Society General Meeting; July 24-28, 2011; Detroit, MI: IEEE.
18. Tang ZR, Li H, Xu FW, Shu Q, Jiang Y. A harmonic impedance estimation method based on the Cauchy mixed model. *Math Probl Eng.* 2020.
19. Liao H, Niebur D. Load profile estimation in electric transmission networks using independent component analysis. *IEEE Trans Power Syst.* 2003;18(2):707-715.

20. Zhao X, Yang HG. A new method to calculate the utility harmonic impedance based on FastICA. *IEEE Trans Power Delivery*. 2015;31(1):381-388.
21. Karimzadeh F, Esmaeili S, Hosseinian SH. Method for determining utility and consumer harmonic contributions based on complex independent component analysis. *IET Gener Transm Distrib*. 2016;10(2):526-534.
22. Zhao JS, Yang HG, Pan AQ, Xu FW. An improved complex ICA based method for wind farm harmonic emission levels evaluation. *Electr Power Syst Res*. 2020;179:106105.
23. Xiao XY, Zheng X, Wang Y, Xu ST, Zheng ZX. A method for utility harmonic impedance estimation based on constrained complex independent component analysis. *Energies*. 2018;11(9):2247.
24. Yu XC, Hu D, Xu J. *Blind Source Separation: Theory and Applications*. New York: John Wiley & Sons; 2013.
25. Lu W, Rajapakse JC. Approach and applications of constrained ICA. *IEEE Trans Neural Network*. 2005;16(1):203-212.

How to cite this article: Zheng X, Xiao X, Wang Y. An impedance matrix constrained-based method for harmonic emission level estimation. *Int Trans Electr Energ Syst*. 2020;e12479. <https://doi.org/10.1002/2050-7038.12479>